西北工業大學
NORTHWESTERN POLYTECHNICAL UNIVERSITY

The OpenFOAM Calculation of Subsonic-Supersonic Shear Mixing Layer

Yang Liu, Ben-shuai Fu

Science and Technology on Combustion, Internal Flow and Thermal-structure Laboratory,

School of Astronautics,

Northwestern Polytechnical University

The 13th OpenFOAM Workshop (OFW13), June 24-29, 2018, Shanghai, China

Contents

- 1. Introduction
- 2. Numerical simulation
- 3. Calculation results of Changing parameters
- 4. Conclusion

1. Introduction

Rocket airflow
Ram airflow
→ Momentum and energy transfer difficulty
→ Affected the performance of combined engine seriously

High-speed, high temperature flow
Low-speed secondary flow
→ Mixing layer develops extreme slow

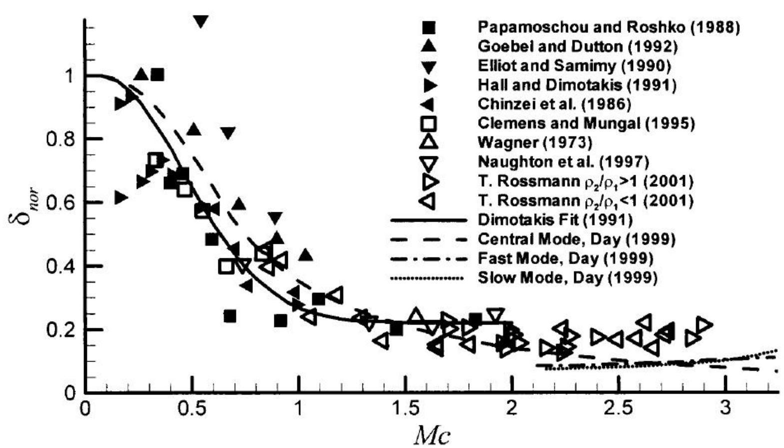

Figure1: Comparison of the results of previous studies on the growth rate of compressible shear mixing layer

It is very essential to carry out research on the development rule of the subsonic-supersonic shear mixing layer.

2. Numerical simulation

2.1 Calculation parameters

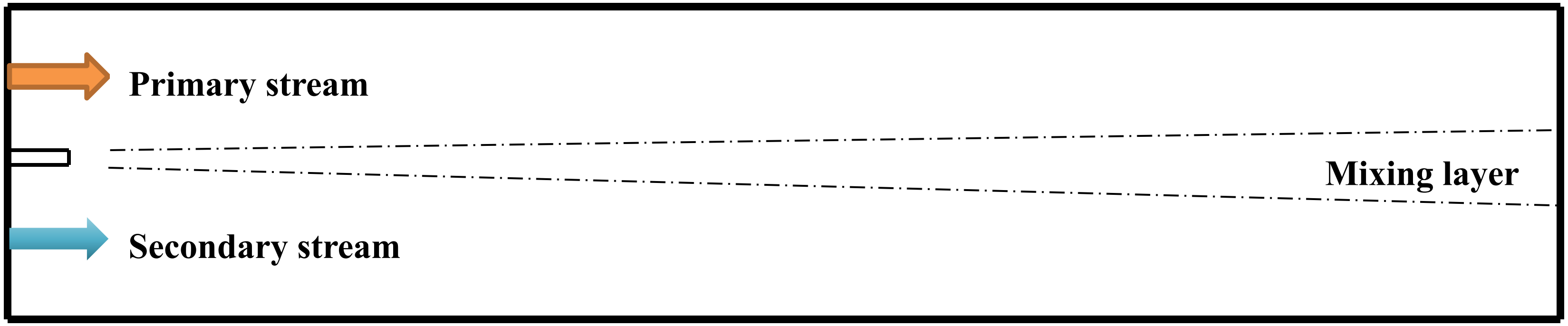

Figure 2 : Schematic diagram of flow area.

Velocity and static temperature are given at high speed and low speed inlet.
Given static pressure at the high speed inlet, the low speed inlet pressure is obtained by extrapolation.
The export condition is zero-gradient boundary condition.
The split board is non-slip, the upper and lower wall is slip.

2. Numerical simulation

2.1 Calculation parameters

The numerical simulation work of subsonic-supersonic shear mixing flow is carried out based on OpenFOAM platform, and using rhoCentralFoam compressible solver, which is a compressible density solver, which has good adaptability for compressible flow.

Table 1: Calculation parameters.

	U1(m/s)	U2(m/s)	Ma1	Ma2	Mc
Case1	517.61	103.24	2	0.3	0.69
Case2	517.61	201.22	2	0.6	0.53
Case3	517.61	289.90	2	0.9	0.39

Keeping the other parameters constant and changing Ma of the secondary flow, studying the effect of Mc on compressibility of shear mixing layer.

2. Numerical simulation

2.2 Numerical validation

Experimental data of normal temperature subsonic-supersonic shear mixing layer carried out by Goebel is adopted for numerical validation. Figure 3 shows the shear mixing layer velocity profile expressed in self-similar form, and it can be found that numerical result is in good agreement with experiment data.

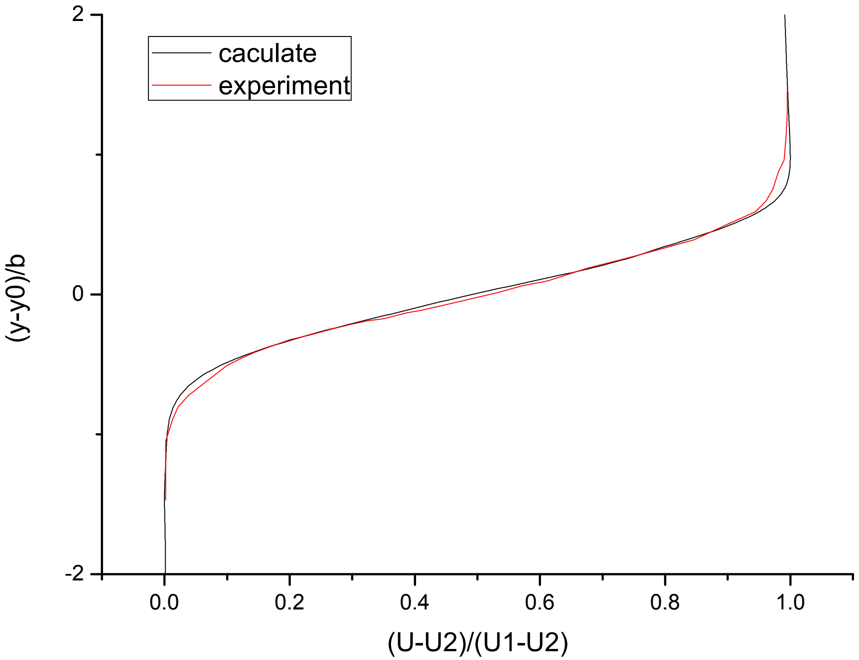

Figure 3: Comparison of shear mixing layer velocity profile between numerical result and experimental data.

2. Numerical simulation

2.3 Calculation results

In the calculation process, when the shear mixing flow reaches the quasi-steady state, the data of a certain moment is selected to obtain the temperature contour. Figure 4 shows the temperature contour of each groups Case1-Case3.

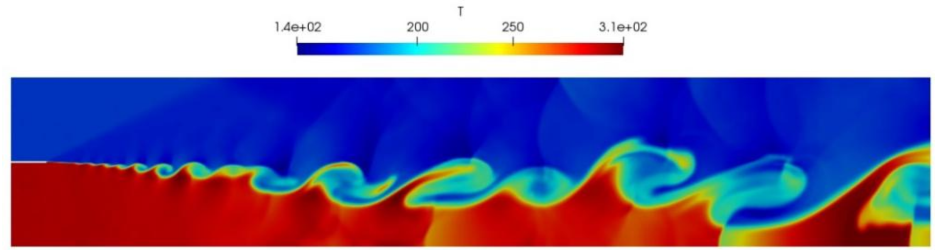

(a) Static temperature distribution contour of Case1.

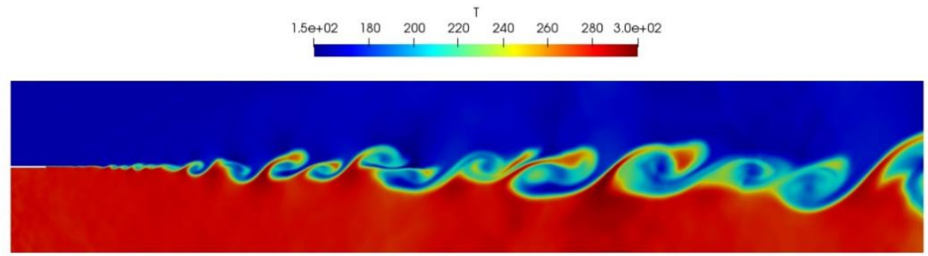

(b) Static temperature distribution contour of Case2.

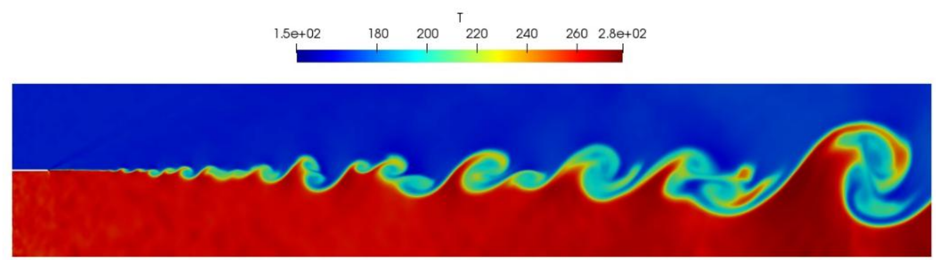

(c) Static temperature distribution contour of Case3.

Figure 4: Static temperature distribution contours of Case1-Case3.

2. Numerical simulation

2.3 Calculation results

The numerical schlieren contour can be obtained by calculating the gradient of the density distribution of the flow field, as shown in the figure 5.

(a) Numerical schlieren contour of Case1.

(b) Numerical schlieren contour of Case2.

(c) Numerical schlieren contour of Case3.

Figure 5: Numerical schlieren contours of Case1-Case3.

2. Numerical simulation

2.3 Calculation results

$$U^*(y) = \frac{U(y)-U_2}{U_1-U_2}$$

$$\delta_{nor} = \frac{(d\delta/dx)}{(d\delta/dx)_{inc}} = f(M_c)$$

$$\left(\frac{d\delta}{dx}\right)_{inc} = C_\delta \frac{(1-r)(1+\sqrt{s})}{2(1+r\sqrt{s})}\left\{1 - \frac{(1-\sqrt{s})/(1+\sqrt{s})}{1+2.9(1+r)/(1-r)}\right\}$$

Figure 6: Thickness of shear mixing layer of Case1-Case3.

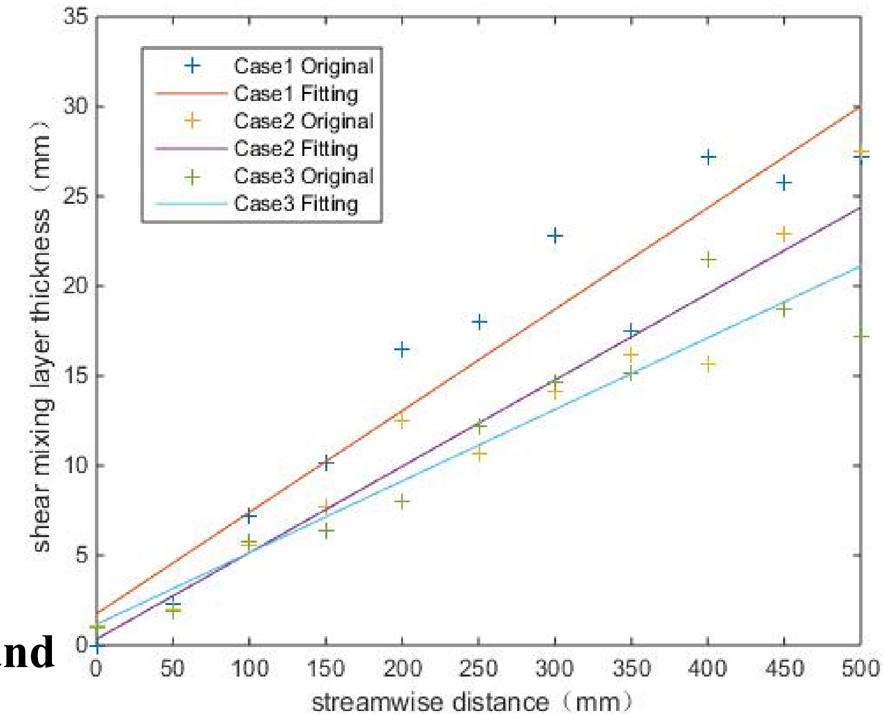

Table 2: Shear layer thickness growth rate and corresponding Mc of Case1-Case3.

	Case1	Case2	Case3
δ'	0.0565	0.0481	0.0399
δ_0'	0.2078	0.1433	0.0948
δ'/δ_0'	0.2720	0.3356	0.4209
Mc	0.69	0.53	0.39

3. Calculation results of Changing parameters

3.1 Different static pressure

In this section, based on Case3, the static pressure of the incoming flow was changed to compare the thickness growth rate of subsonic-supersonic shear mixing layer under different static pressure conditions.

Table 3: Calculation parameters.

	Ma1	Ma2	Mc	static pressure (kPa)
B1	2	0.3	0.39	36
B2	2	0.3	0.39	60
B3	2	0.3	0.39	100

3. Calculation results of Changing parameters

3.1 Different static pressure

In the calculation process, when the shear mixing flow reaches the quasi-steady state, the data of a certain moment is selected to obtain the density distribution of flow field. The numerical schlieren contour can be obtained by calculating the gradient of the density distribution of the flow field, as shown in the figure 7.

(a) Numerical schlieren contour of B1.

(b) Numerical schlieren contour of B2.

(c) Numerical schlieren contour of B3.

Figure7: Numerical schlieren contours of B1-B3.

3. Calculation results of Changing parameters

3.1 Different static pressure

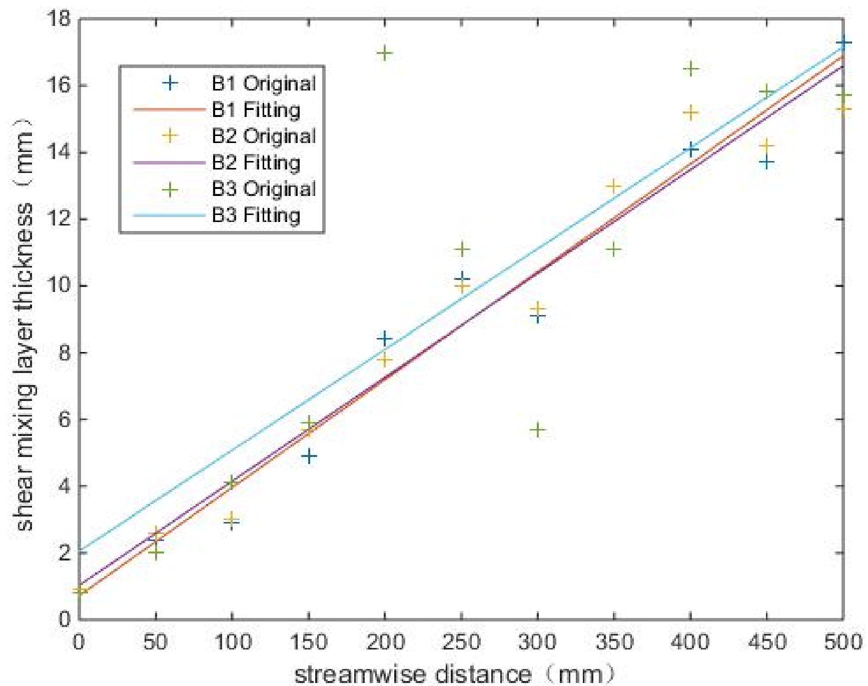

Figure 8: Thickness of shear mixing layer of B1-B3.

Table 4: Shear layer thickness growth rate and corresponding Mc of B1-B3.

	B1	B2	B3
δ'	0.0323	0.0311	0.0302
δ'_0	0.0948	0.0948	0.0948
δ'/δ'_0	0.3407	0.3281	0.3183
static pressure (kPa)	36	60	100

3. Calculation results of Changing parameters

3.2 Different airflow quality

In this section, based on Case3, the airflow quality of the incoming flow was changed to compare the thickness growth rate of subsonic-supersonic shear mixing layer under different airflow quality.

Table 5: Calculation parameters.

	Ma1	Ma2	Mc	split board length
C1	2	0.3	0.39	20mm
C2	2	0.3	0.39	50mm
C3	2	0.3	0.39	100mm

3. Calculation results of Changing parameters

3.2 Different airflow quality

In the calculation process, when the shear mixing flow reaches the quasi-steady state, the data of a certain moment is selected to obtain the density distribution of flow field. The numerical schlieren contour can be obtained by calculating the gradient of the density distribution of the flow field, as shown in the figure 9.

(a) Numerical schlieren contour of C1.

(b) Numerical schlieren contour of C2.

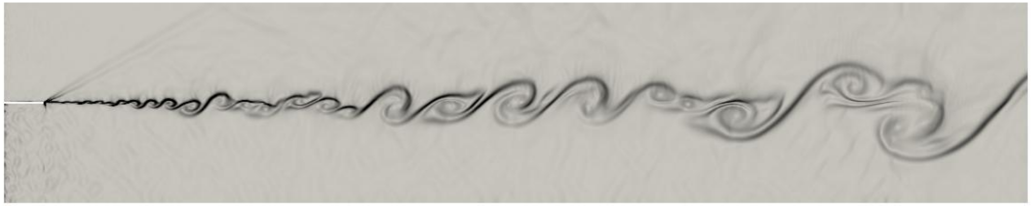

(c) Numerical schlieren contour of C3.

Figure 9: Numerical schlieren contours of C1-C3.

3. Calculation results of Changing parameters

3.2 Different airflow quality

Figure 10: Thickness of shear mixing layer of C1-C3.

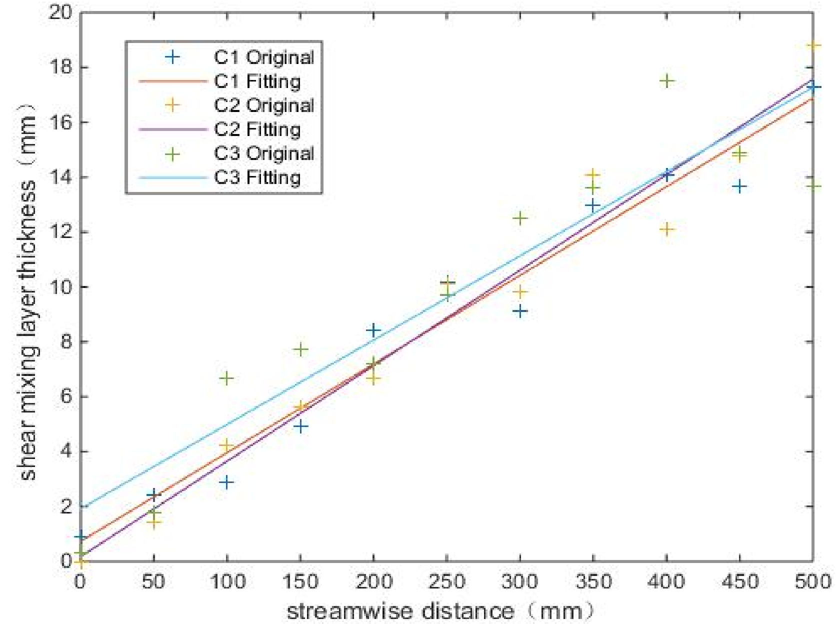

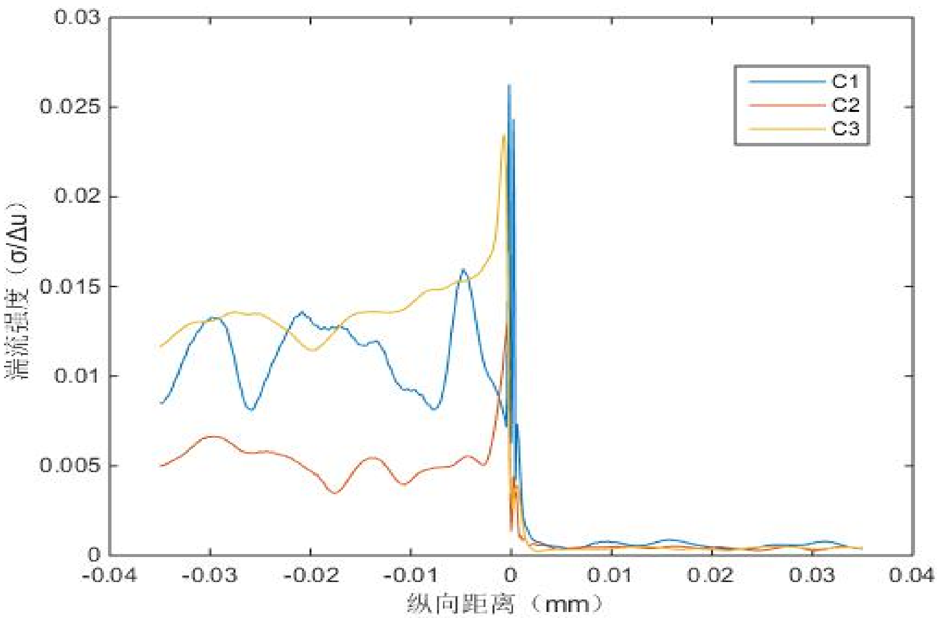

Figure 11: Thickness of shear mixing layer of C1-C3

3. Calculation results of Changing parameters

3.2 Different airflow quality

Table 6: Shear layer thickness growth rate and corresponding Mc of C1-C3.

	C1	C2	C3
δ'	0.0323	0.0348	0.0307
δ'_0	0.0948	0.0948	0.0948
δ' / δ'_0	0.3407	0.3670	0.3238
the order of turbulence intensity	2	3	1

It can be seen from the above table, both dimensionless thickness growth rate and thickness growth rate of shear mixing layer decrease with the increase of turbulence intensity.

4.Conclusion

- **In view of the subsonic-supersonic shear mixing flow, this paper uses the software of OpenFOAM to carry out large eddy simulation study, and the results show that the development process of the subsonic-supersonic shear mixing layer has the following rules:**
- **(1) With the increase of compressibility, the dimensionless thickness growth rate of the shear mixing layer decreases.**
- **(2) With the increase of static pressure, both dimensionless thickness growth rate and thickness growth rate of shear mixing layer decrease.**
- **(3) With the increase of turbulence intensity, both dimensionless thickness growth rate and thickness growth rate of shear mixing layer decrease.**

Thank you for your attention!